Journal of the European Ceramic Society 22 (2002) 219–223

www.elsevier.com/locate/jeurceramsoc

Phase developments and dielectric/ferroelectric responses in the PMN–PT system

Dong-Hwan Suh, Dong-Ha Lee, Nam-Kyoung Kim*

Department of Inorganic Materials Engineering, Kyungpook National University, Taegu 702-701, South Korea

Received 11 January 2001; accepted 26 March 2001

Abstract

Monophasic ($\geqslant 99.4\%$) perovskite powders of a $Pb(Mg_{1/3}Nb_{2/3})O_3$–$PbTiO_3$ system were prepared by a B-site precursor method. Phase developments and lattice parameter changes in the perovskite system were examined by X-ray diffraction. Weak-field dielectric responses of the ceramic system were investigated as functions of $PbTiO_3$ concentration and measurement frequency. Phase transition modes in the dielectric spectra were analyzed in terms of diffuseness characteristics. Ferroelectric hysteresis behaviors were monitored with respect to temperature changes.

Keywords: Dielectric properties; Ferroelectric properties; Perovskites; PMN–PT; X-ray methods

1. Introduction

Lead magnesium niobate [$Pb(Mg_{1/3}Nb_{2/3})O_3$, PMN], a prototype relaxor ferroelectric, demonstrates a quite high maximum dielectric constant around $-10\sim-5°C$, with diffuse phase transition (DPT) phenomena.[1–4] In contrast, a normal ferroelectric compound of lead titanate ($PbTiO_3$, PT) exhibits a sharp phase transition (SPT) mode, with a very high dielectric maximum temperature of $\sim 490°C$. Whereas preparation of perovskite PMN by a conventional mixed-oxide process is usually accompanied by unwanted formation of Pb–(Mg–)Nb–O pyrochlore phase(s), perovskite PT can be synthesized readily from constituent chemicals.

So far, the PMN–PT system has been extensively studied.[5–11] Most of the results, however, have focused on the dielectric, pyroelectric, electrostrictive properties, and/or structural studies, especially near the morphotropic phase boundary (MPB). In the present study, PMN and PT (with quite different modes in the phase transition behavior) were again chosen as end components and selected compositions in the (pseudo)binary system were prepared. Unlike previous reports, however, phase transition modes between the diffuse (second-order) and sharp (first-order) dielectric constant spectra were closely investigated in terms of diffuseness characteristics. Phase developments and lattice parameter changes as well as ferroelectric responses were also examined. In order to enhance the perovskite formation, the system powders were prepared by a "B-site precursor method,"[12,13] which is a more-inclusive term of the well-known "columbite process."[14,15]

2. Experimental procedure

The system under investigation is $(1-x)Pb(Mg_{1/3}Nb_{2/3})O_3$–$xPbTiO_3$ (or $(1-x)$PMN$-x$PT in short), with values of x ranging from 0.0 to 1.0 at regular steps of 0.2. Additionally, the interval between $x=0.2$ and 0.4 was subdivided into 0.05 increments for extensive characterization of the crystallographic aspects as well as dielectric properties. Starting materials were oxide chemicals of PbO (purity > 99.5%), MgO (99.9%), Nb_2O_5 (99.9%), and TiO_2 (99.9%). In order to maintain stoichiometries as closely to the nominal compositions as possible, moisture contents of raw chemicals and prepared precursors were measured and introduced into the batch calculations.

B-site precursor batches of $(1-x)(Mg_{1/3}Nb_{2/3})O_2$–$x$ TiO_2 (or $[(Mg_{1/3}Nb_{2/3})_{1-x}Ti_x]O_2$), except for the extreme composition of $x=1.0$ (TiO_2), were prepared by

* Corresponding author. Tel.: +82-53-950-5636; fax: +82-53-950-5645.

E-mail address: nkkim@knu.ac.kr (N.-K. Kim).

0955-2219/01/$ - see front matter
PII: S0955-2219(01)00278-3

weighing required proportions of constituent chemicals. The powders were milled under alcohol, dried, calcined at 1150°C for 2 h in a covered alumina crucible and were examined by X-ray diffraction (XRD) to identify the phase(s) formed. The precursor powders were then mixed with PbO (without any addition of excess amount), milled, dried and calcined at 800–850°C to form the perovskite system. Phase identification was again carried out by XRD.

The perovskite powders were mixed with an aqueous solution (2 wt.%) of polyvinyl alcohol and pressed isostatically into pellets at 100 MPa. The samples were sintered at 1200–1250°C for 1 h in a multiple-enclosure crucible setup.[16] In order to maintain lead atmosphere during the firing process, sample pellets were embedded in the perovskite powders of identical composition. After grinding/polishing to attain parallel sides, bulk densities of the pellets were measured geometrically, followed by gold sputtering and overcoating with silver paste for electrical contacts. Dielectric constants were measured using an impedance analyzer (10^{3-6} Hz, ~ 1 V_{rms}/mm) on cooling. Polarization behaviors of the ceramics were also examined using a ferroelectric test system.

3. Results and discussion

X-ray profiles of the B-site precursor system $[(Mg_{1/3}Nb_{2/3})_{1-x}Ti_x]O_2$ are contrasted in Fig. 1(a). The diffractogram of $x=0.0$ matched exactly that of columbite $MgNb_2O_6$ (ICDD No. 33-875), whereas that of $x=1.0$ is of a rutile structure of TiO_2 (ICDD No. 21-1276). In the latter pattern, however, several extraneous reflections of anatase (ICDD No. 21-1272; denoted by Δ) were also detected, though only of a negligibly small intensity. Reflections of the columbite structure are also observable at $x \leqslant 0.4$, whereas those of the rutile persisted down to $x=0.2$. Therefore, the two structures coexisted at intermediate compositions of $x=0.2$–0.4, indicating that the columbite and rutile did not develop complete solubilities due to dissimilar structures. Meanwhile, distinct increases in the reflection angles (e.g. those of 27–28°, 35–36°, and 53–55°) with increasing values of x are noticeable, which is undoubtedly attributed to the gradual replacement of $Mg_{1/3}Nb_{2/3}$ complex (weighted average radius = 0.0667 nm)[17] by Ti (0.0605 nm)[17] and accompanying contraction of the crystalline lattices.

In the XRD spectra of the $(1-x)$PMN–xPT system, Fig. 1(b), that of $x=1.0$ (PT) is indexed according to a tetragonal symmetry of perovskite. The patterns at low values of x, however, are apparently of a (pseudo)cubic symmetry. Since no trace of unreacted Nb_2O_5 could be identified throughout the B-site precursor system [Fig. 1(a)], formation chances of the pyrochlore(s) could have been minimal. As a result, only a perovskite structure (with negligible amounts of parasitic pyrochlore)

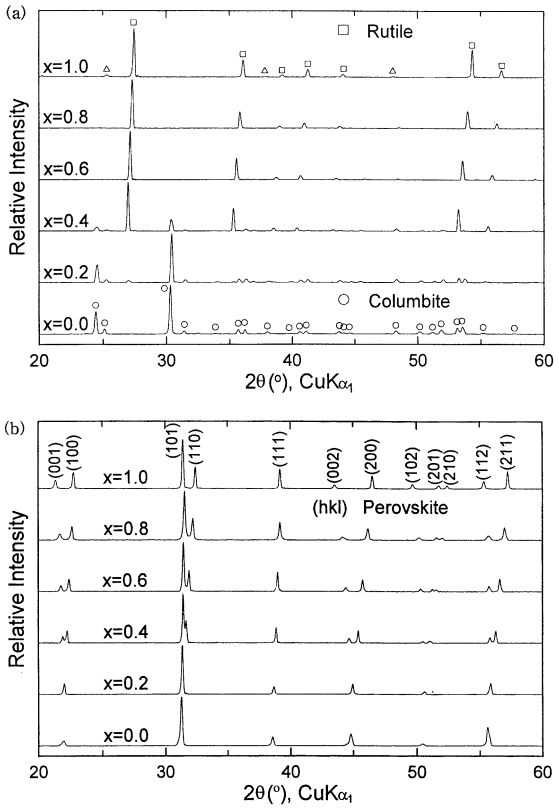

Fig. 1. Room temperature X-ray patterns of (a) $(1-x)(Mg_{1/3}Nb_{2/3})O_2$–$xTiO_2$ and (b) $(1-x)Pb(Mg_{1/3}Nb_{2/3})O_3$–$xPbTiO_3$ powders.

was detected throughout the entire system, with phase yields of >99.4%. Effectiveness of the B-site precursor method in suppression of the pyrochlore formation during perovskite development has thus been proven again in the present study, as powders of such high purities (especially at PMN-rich compositions) are unattainable by conventional one-step mixed-oxide processes. Promotion of the perovskite development by PT introduction has also been reported in the systems of $Pb[(Mg,Zn)_{1/3}(Ta,Nb)_{2/3}]O_3$.[18–22]

Lattice parameters of the perovskite structure were calculated from the XRD data and the results are compared in Fig. 2, along with tetragonality factors (or axial ratios of c/a) and average lattice parameters of $(a^2c)^{1/3}$. The parameters of (pseudo)cubic PMN ($x=0.0$) and tetragonal PT ($x=1.0$) are 0.4046 nm, and $a=0.3897$ and $c=0.4151$ nm, respectively, which are virtually identical to reported data (ICDD Nos. 27-1199 and 6-452). The (pseudo)cubic symmetry of PMN was maintained up to $x=0.3$. At $x=0.4$, however, peak splittings are well defined in Fig. 1(b), with $a=0.3992$ nm, $c=0.4051$ nm, and $c/a=1.015$. From the crystallographic analyses, therefore, the phase boundary between the (pseudo)cubic and tetragonal symmetries seems to be located at $x=0.3$–0.35. The composition range is in good agreement with $x=0.29$–0.32,[8] $x=0.30$–0.325,[5,6] $x=0.345$,[10,11] and $x \cong 0.35$,[9] but is somewhat

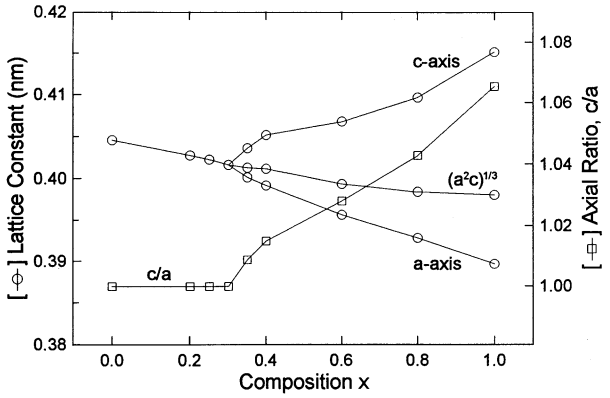

Fig. 2. Lattice parameters [a- and c-axis, and $(a^2c)^{1/3}$] and tetragonality factors (c/a) of the $(1-x)$PMN–xPT system.

lower than $x \cong 0.4$.[23] With further increases in x, the a-axis shrunk while the c-axis expanded continuously at approximately similar rates. Consequently, the values of $(a^2c)^{1/3}$ decreased slowly, while the axial ratios of c/a increased rapidly to 1.065. By comparing the B-site cation sizes of PMN and PT (0.0667 vs. 0.0605 nm),[17] the continuous decrease in the average lattice parameter (from 0.4046 nm at $x=0.0$ to 0.3980 nm at $x=1.0$) can be well understood, which supports the formation of complete crystalline solutions of a perovskite structure.

Since pure PT could not be prepared as a bulk form of high density, the composition of $x=1.0$ could not be examined any further for the rest of the study. The comparatively large c/a value of 1.065 ($x=1.0$, PT) is identical to a reported value (ICDD No. 6-452) and is responsible for the frequent crack developments around the phase transition temperature during cooling of fired pieces. Relative densities of the sintered pellets were 93–96% of the theoretical values.

Dielectric constant spectra of sintered ceramics in the $(1-x)$PMN–xPT system are shown in Fig. 3. The spectra of $0.2 \leqslant x \leqslant 0.4$ at 10, 100, and 1000 kHz are purposefully omitted for simplicity. Maximum dielectric constants (K_{max}) of $x=0.0$ (PMN) were heavily dependent upon frequency: 19,900 (1 kHz), 18,400 (10 kHz), 16,900 (100 kHz), and 15,100 (1 MHz). In contrast, those of $x=0.6$ (0.4PMN–0.6PT) were 17,000–18,000, regardless of the measurement frequency. The two sets of spectra, therefore, are quite contrasting in that the former composition exhibited a rather diffuse mode in the phase transition (typical of relaxor ferroelectrics), whereas the latter showed a much different mode of SPT character.

It is interesting to note that maximum values in the dielectric spectra at $x=0.2$–0.4 were nearly constant, $\leqslant 30{,}000$. On the other hand, the dielectric maximum temperatures in the same composition range increased progressively from 97 to 202°C, which are quite close to those reported by Choi et al.[5,6] The temperatures, however, are substantially different (by up to ~20°C) from the results of three separate groups of Kuwabara et al.,[7] Bossler et al.,[24] and Kelly et al.,[11] even when small differences in the composition (by up to 2–2.5 mol%) are considered. Similarly, the maximum dielectric constants in the present study are somewhat different from those of the three groups: the values by the first and second groups are only 40–60% of the present results, while those by the third group are 110–160%. Such wide discrepancies in the dielectric data are believed to have originated from the methods of powder preparation: B-site precursor method (Kelly et al. and present study) vs. direct-mixing of PMN and PT powders (Kuwabara et al.) or one-step calcining-mixed-oxide process (Bossler et al.).

Frequency-dependent dielectric maximum temperatures (T_{max}) of the perovskite system are plotted in Fig. 4 in two different ways. The temperatures of PMN were −5°C (1 kHz), 0°C (10 kHz), 5°C (100 kHz), and 12°C (1 MHz), whereas those of $x=0.3$ (0.7PMN–0.3PT) were 153–154°C (1–1000 kHz). T_{max} values of the entire system increased fairly linearly with increasing PT concentration, with an average gradient of 5.0°C/mol% PT at 1 kHz. The increasing rate is in excellent agreement with the value obtained from the difference (~500°C) in

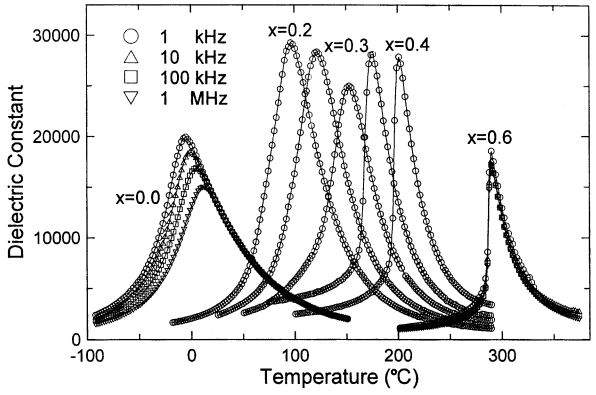

Fig. 3. Dielectric constant spectra of the $(1-x)$PMN–xPT system ceramics.

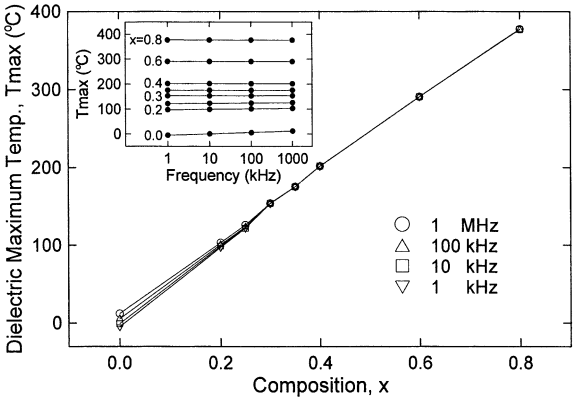

Fig. 4. Variations of the dielectric maximum temperature with changes in composition and measurement frequency.

the dielectric maximum temperatures of PMN and PT. Meanwhile, frequency-dependent dispersion of PMN is quite substantial, i.e. $\Delta T_{max}(=T_{max,1\ MHz}-T_{max,1\ kHz})=17°C$, but the value immediately became smaller to $\sim 2°C$ ($x=0.2$) and virtually negligible ($\leqslant 1°C$) at $0.3\leqslant x$. The rapid decrease in the dielectric dispersion is well demonstrated in the inset.

In order to evaluate the intermediate modes of phase transition between the sharp and diffuse types (as reflected in the dielectric constant spectra), an empirical power form of comprehensive equation (comprising the Curie–Weiss law and quadratic relation)[25] was introduced as $1/K=1/K_{max}+(T-T_{max})^{\gamma}/C$.[7,26] Two quantitative measures of relative broadness (or diffuseness) in the dielectric spectra are the diffuseness exponent (γ) and degree of diffuseness (C/K_{max}), detailed physical meanings and derivation methods of which can be found elsewhere.[4,26–28]

Relationships of $\log(1/K-1/K_{max})$ vs. $\log(T-T_{max})$ are presented in Fig. 5, together with the variations of the two diffuseness parameters shown in the inset. The diffuseness exponent for $x=0.0$ (PMN) was $\gamma=1.67$, which is very close to a reported value of 1.64[26] but much smaller than 2.0.[7] By comparison, a somewhat larger value of $\gamma=1.76$ was reported for $Pb(Mg_{1/3}Ta_{2/3})O_3$ (PMT)[28] and $Pb(Zn_{1/3}Nb_{2/3})O_3$ (PZN).[26] As summarized in the inset, the phase transition modes changed from diffuse to sharp ones with increasing PT concentration in general. The diffuseness exponent, however, was maximized to $\gamma=1.90$ ($x=0.25$) near the MPB range, followed by a steady decrease to 1.18 at $x=0.6$. The trend of overall decrease in the diffuseness exponents (except for the MPB region) could also be found in many PT-substituted systems of PMT,[21] PMN,[7] $Pb(Zn_{1/3}Ta_{2/3})O_3$,[22] and unmodified[20] and PMN-modified[29] PZN. Variation of the degree of diffuseness was similar to that of the diffuseness exponent.

Dependencies of the remnant and spontaneous polarization (P_r and P_s) and coercive field (E_C) of a representative composition $x=0.2$ (0.8PMN–0.2PT) upon temperature are displayed in Fig. 6. Note that the coercive fields are drawn with a descending scale in order to avoid a congested appearance. In general, the three variables decreased continuously in magnitudes with increasing temperature. In detailed observations, however, E_C decreased nearly linearly from 6.9 kV/cm at −33°C to negligible values at temperatures slightly (by ~20°C) below the phase transition. Similarly, P_r decreased from 20 $\mu C/cm^2$ (−33°C) at a slow rate initially, followed by steep decline to near-zero values in the same temperature range. In contrast, P_s of 23 $\mu C/cm^2$ (−33°C) decreased rather slowly and substantial values were still retained at temperatures well above the phase transition, e.g. 3.8 $\mu C/cm^2$ at 177°C. The smearing trend in the spontaneous polarization, together with sharp decreases in the remnant polarization and coercive field (especially near the phase transition region), is usually observed in relaxor ferroelectric compositions.[30–32]

4. Summary

In the B-site precursor system of $(1-x)(Mg_{1/3}Nb_{2/3})O_2$–$xTiO_2$, columbite and rutile structures were detected at low and high values of x, respectively, with a narrow range of limited solid solubilities developed at intermediate compositions. In the $(1-x)$PMN–xPT system, in contrast, a continuous series of perovskite solid solution was formed. The lattice parameter of the (pseudo)-cubic perovskite PMN was 0.4046 nm, while those of the tetragonal perovskite PT were $a=0.3897$ and $c=0.4151$ nm. With increasing PT concentration in the range of $x=0.3$–1.0, the tetragonality factors increased rapidly (~1.000→1.065), whereas values of the average lattice parameter decreased steadily (0.4016→0.3980 nm). Dielectric constant spectra of the PMN-rich compositions (i.e. low values of x) showed typical relaxation behaviors of frequency dependence (e.g. $\Delta T_{max}=17°C$ at $x=0.0$) with diffuse phase transition modes. With increasing PT concentration, the dielectric maximum

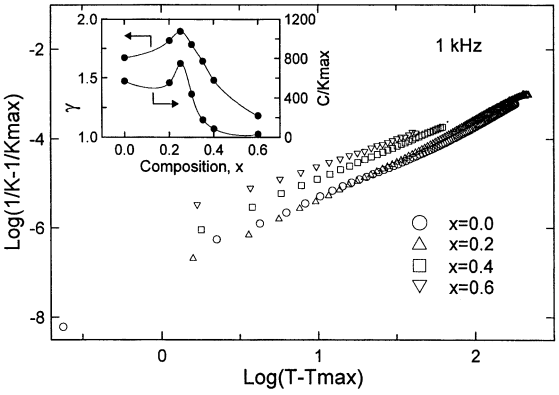

Fig. 5. $\log(1/K-1/K_{max})$ vs. $\log(T-T_{max})$ for the analyses of γ and C/K_{max}.

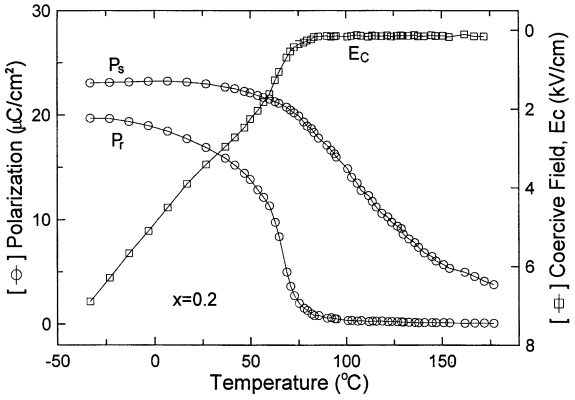

Fig. 6. Temperature-dependent values of the remnant/spontaneous polarization and coercive field at $x=0.2$.

temperatures increased nearly linearly, while ΔT_{max} became smaller and eventually negligible at $0.3 \leqslant x$. Diffuseness parameters in the dielectric constant spectra turned out not to be linear functions of the PT concentration, but were maximized near the MPB compositions instead. In the ferroelectric hysteresis responses, remnant polarizations and coercive fields decreased sharply (especially near the phase transition temperature range), whereas values of the spontaneous polarization decreased rather smoothly with increasing temperature, as is typical of relaxor ferroelectrics.

Acknowledgements

This work was supported by the Korea Science and Engineering Foundation (KOSEF) through the Center for Interface Science and Engineering of Materials (CISEM) at Korea Advanced Institute of Science and Technology (KAIST). The authors wish to acknowledge the financial support of the Korea Research Foundation made in the program year 1998 (D00010).

References

1. Katayama, K., Abe, M., Akiba, T. and Yanagida, H., Sintering and dielectric properties of single-phase $Pb(Mg_{1/3}Nb_{2/3})O_3$–$PbTiO_3$. *J. Eur. Ceram. Soc.,* 1989, **5**(3), 183–191.
2. Yamashita, Y., Relaxor ceramic dielectric materials for multilayer ceramic capacitors. In *Proceedings of the Seventh IEEE International Symposium on Applications of Ferroelectrics*, 1990, pp. 241–245.
3. Chae, M.-C. and Kim, N.-K., Perovskite formation by B-site precursor method and dielectric characteristics of $Pb[Mg_{1/3}(Ta,Nb)_{2/3}]O_3$ ceramic system. *Ferroelectrics,* 1998, **209**(3/4), 603–613.
4. Chae, M.-C., Lim, S.-M. and Kim, N.-K., Stabilization of perovskite phase and enhancement in dielectric properties by substitution of $Pb(Mg_{1/3}Nb_{2/3})O_3$ to $Pb(Zn_{1/3}Ta_{2/3})O_3$. *Ferroelectrics,* 2000, **242**(1–4), 25–35.
5. Choi, S. W., Shrout, T. R., Jang, S. J. and Bhalla, A. S., Morphotropic phase boundary in $Pb(Mg_{1/3}Nb_{2/3})O_3$–$PbTiO_3$ system. *Mater. Lett.,* 1989, **8**(6/7), 253–255.
6. Choi, S. W., Shrout, T. R., Jang, S. J. and Bhalla, A. S., Dielectric and pyroelectric properties in the $Pb(Mg_{1/3}Nb_{2/3})O_3$–$PbTiO_3$ system. *Ferroelectrics,* 1989, **100**, 29–38.
7. Kuwabara, M., Takahashi, S., Goda, K., Oshima, K. and Watanabe, K., Continuity in phase transition behavior between normal and diffuse phase transitions in complex perovskite compounds. *Jpn. J. Appl. Phys.,* 1992, **31**(9B), 3241–3244.
8. Ho, J. C., Liu, K. S. and Lin, I. N., Study of ferroelectricity in the PMN–PT system near the morphotropic phase boundary. *J. Mater. Sci.,* 1993, **28**(16), 4497–4502.
9. Bunina, O., Zakharchenko, I., Yemelyanov, S., Timonin, P. and Sakhnenko, V., Phase transitions in $PbMg_{1/3}Nb_{2/3}O_3$–$PbTiO_3$ system. *Ferroelectrics,* 1994, **157**(1–4), 299–303.
10. Kelly, J., Farrey, G. and Safari, A., A comparison of the properties of (1−x)PMN–xPT ceramics near the morphotropic phase boundary prepared by sol–gel and columbite precursor methods. In *Proceedings of the Tenth IEEE International Symposium on Applications of Ferroelectrics*, ed. B. M. Kulwicki, A. Amin and A. Safari. IEEE, Piscataway, NJ, 1996, pp. 699–702.
11. Kelly, J., Leonard, M., Tantigate, C. and Safari, A., Effect of composition on the electromechanical properties of $(1-x)Pb(Mg_{1/3}Nb_{2/3})O_3$–$xPbTiO_3$ ceramics. *J. Am. Ceram. Soc.,* 1997, **80**(4), 957–964.
12. Lee, B.-H., Kim, N.-K., Kim, J.-J. and Cho, S.-H., Perovskite formation sequence by B-site precursor method and dielectric properties of PFW–PFN ceramics. *Ferroelectrics,* 1998, **211**(1–4), 233–247.
13. Lee, B.-H., Kim, N.-K. and Park, B.-O., Perovskite formation and dielectric characteristics of $PFW_{0.2}$•$PFT_{0.8-x}$•PFN_x system ceramics. *Ferroelectrics,* 1999, **227**(1–4), 87–96.
14. Swartz, S. L. and Shrout, T. R., Fabrication of perovskite lead magnesium niobate. *Mater. Res. Bull.,* 1982, **17**(10), 1245–1250.
15. Swartz, S. L., Shrout, T. R., Schulze, W. A. and Cross, L. E., Dielectric properties of lead magnesium niobate ceramics. *J. Am. Ceram. Soc.,* 1984, **67**(5), 311–315.
16. Chae, M.-C., Kim, N.-K., Kim, J.-J. and Cho, S.-H., Preparation and dielectric properties of $Pb[(Mg_{1/3}Ta_{2/3}),(Zn_{1/3}Nb_{2/3})]O_3$ relaxor ceramics. *Ferroelectrics,* 1998, **211**(1–4), 25–39.
17. Shannon, R. D., Revised effective ionic radii and systematic studies of interatomic distances in halides and chalcogenides. *Acta Crystall,* 1976, **A32**(5), 751–767.
18. Kim, Y. J. and Choi, S. W., Dielectric and pyroelectric properties in the $Pb(Mg_{1/3}Ta_{2/3})O_3$–$PbTiO_3$ solid solution ceramics. *Ferroelectrics,* 1990, **108**, 241–246.
19. Choi, S. W. and Jung, J. M., Morphotropic phase boundary in $Pb(Mg_{1/3}Ta_{2/3})O_3$–$PbTiO_3$ system. *J. Kor. Phys. Soc.,* 1996, **29**(Suppl.), S672–S675.
20. Lee, D.-H. and Kim, N.-K., Crystallographic, dielectric, and diffuseness characteristics of PZN-PT ceramics. *Mater. Lett.,* 1998, **34**(3–6), 299–304.
21. Kim, J.-S. and Kim, N.-K., Lead magnesium tantalate–lead titanate perovskite ceramic system: preparation and characterization. *Mater. Res. Bull.,* 2000, **35**(14), 2479–2489.
22. Kim, J.-S., Kim, N.-K. and Kim, H., Perovskite developments in $Pb(Zn_{1/3}Ta_{2/3})O_3$ with $PbTiO_3$ substitution and dielectric characteristics. *J. Mater. Res.*, submitted for publication.
23. Ouchi, H., Nagano, K. and Hayakawa, S., Piezoelectric properties of $Pb(Mg_{1/3}Nb_{2/3})O_3$–$PbTiO_3$–$PbZrO_3$ solid solution ceramics. *J. Am. Ceram. Soc.,* 1965, **48**(12), 630–635.
24. Bossler, F., Escure, P., Lejeune, M. and Mercurio, J. P., Dielectric and piezoelectric properties of $PbMg_{1/3}Nb_{2/3}O_3$–$PbTiO_3$–$PbZn_{1/3}Nb_{2/3}O_3$ ceramics. *Ferroelectrics,* 1993, **138**(1–4), 103–112.
25. Kirillov, V. V. and Isupov, V. A., Relaxation polarization of $Pb(Mg_{1/3}Nb_{2/3})O_3$ — a ferroelectric with a diffuse phase transition. *Ferroelectrics,* 1973, **5**(1/2), 3–9.
26. Uchino, K. and Nomura, S., Critical exponents of the dielectric constants in diffused-phase-transition crystals. *Ferroelectrics Lett.,* 1982, **44**(3), 55–61.
27. Butcher, S. J. and Thomas, N. W., Ferroelectricity in the system $Pb_{1-x}Ba_x(Mg_{1/3}Nb_{2/3})O_3$. *J. Phys. Chem. Solids,* 1991, **52**(4), 595–601.
28. Lim, S.-M. and Kim, N.-K., Perovskite phase developments in $Pb[(Mg,Zn)_{1/3}Ta_{2/3}]O_3$ system and dielectric characteristics. *J. Mater. Sci.,* 2000, **35**(17), 4373–4378.
29. Lee, D.-H., Kim, N.-K. and Ko, J., Perovskite phase developments and dielectric properties of PMN-substituted PZN–PT system. *Mater. Res. Bull.,* 1999, **34**(14/15), 2185–2191.
30. Smolenskii, G. A., Physical phenomena in ferroelectrics with diffused phase transition. *J. Phys. Soc. Jpn.,* 1970, **28** (Suppl.), 26–37.
31. Cross, L. E., Relaxor ferroelectrics. *Ferroelectrics,* 1987, **76**(3/4), 241–267.
32. Cross, L. E., Relaxor ferroelectrics: an overview. *Ferroelectrics,* 1994, **151**(1–4), 305–320.